Angewandte Chemie
Eine Zeitschrift der Gesellschaft Deutscher Chemiker

Supporting Information

69451 Weinheim, Germany

An Octanuclear [$Cr^{III}_4Dy^{III}_4$] 3d–4f Single-Molecule Magnet**

*Julia Rinck, Ghenadie Novitchi, Willem Van den Heuvel, Liviu Ungur, Yanhua Lan, Wolfgang Wernsdorfer, Christopher E. Anson, Liviu F. Chibotaru, and Annie K. Powell**

anie_201002690_sm_miscellaneous_information.pdf

Experimental Section:

Synthesis: Due to the air-sensitivity of the $CrCl_2$ all procedures up to the final crystallisation were carried out under an argon or nitrogen inert gas atmosphere using a Braun glovebox or standard Schlenk technique. The solvents used were dried prior to use. Acetonitrile was dried using calcium hydride and P_2O_5 and stored over molecular sieves (3Å). Dichloromethane was dried from P_2O_5 and stored over molecular sieves (4 Å). $CrCl_2$, *N*-methyldiethanolamine, NaN_3 and pivalic acid were purchased from Acros, Aldrich and/or Fluka and used as received.

A mixture of $CrCl_2$ (0.124 g, 1.00 mmol), NaN_3 (0.110 g, 1.69 mmol) and *N*-methyldiethanolamine (373 µl, 3.55 mmol) in acetonitrile (15 mL) was stirred at room temperature for 50 min. After the addition of $Dy(NO_3)_3 \cdot 6H_2O$ (200 mg, 0.44 mmol) and pivalic acid (400 mg, 3.91 mmol) the mixture was stirred for another 10 min before the addition of dichloromethane (10 mL). The mixture was stirred at room temperature overnight (13 h). The solution was filtered and exposure to air; slow evaporation of the solvent gave pink crystals of **1**.

Yield: 0.137g (20.87 % calc. for Cr)

EA: calc. for $C_{62}H_{126}Cl_4Cr_4Dy_4N_{16}O_{29}$ (corresponds to replacement of one lattice $CHCl_2$ by H_2O): C:29.09 H:4.96 N:8.76; found: C:29.10 H:4.95 N:8.57

IR (KBr): $\tilde{n}$ = 414.88 (m), 454.71 (sh), 482.01 (s), 501.62 (s), 532.95 (s), 583.28 (m), 595.54 (s), 619.92 (s), 659.85 (m), 678.76 (s), 750.08 (s), 793.98 (m), 878.84 (m), 938.12 (w), 1001.67 (s), 1025.82 (sh), 1036.57 (s), 1001.23 (vs), 1149.56 (s), 1228.32 (vs), 1297.75 (s), 1358.68 (s), 1376.01 (vs), 1412.12 (vs), 1458.25 (s), 1484.33 (vs), 1522.90 (w), 1574.13 (vs), 2082.44 (vs), 2346.19 (vw), 2368.62 (vw), 2677.38 (vw), 2695.88 (vw), 2725.76 (vw), 2868.63 (s), 2901.60 (s), 2926.84 (s), 2958.42 (s), 2978.81 (sh), 3403.90 (m) cm^{-1}.

Crystallography:

Data were collected at 100K on a Bruker SMART Apex CCD diffractometer using graphite-monochromated Mo-K_a radiation. Data were corrected for absorption using SADABS.[x] Structure solution by direct methods and full-matrix least-squares refinement against F^2 (all data) were carried out using the SHELXTL package.[y] All ordered non-H atoms were refined anisotropically. Organic H atoms were placed in calculated positions.

The methylene groups of the Me-dea ligands are disordered by a 27 degree rotation about the Dy-N bond, with the two components related by the crystallographic mirror plane, and the atoms were refined with half-occupancy. The t-butyl group of the pivalate ligand was two-fold disordered, with relative occupancies 55:45. The partial carbon atoms could be refined anisotropically with appropriate (DELU) restraints. The lattice dichloromethane molecules were badly disordered, and the data were treated using the SQUEEZE option within PLATON.[z] Electron density corresponding to 276 e was corrected for: calculated for six CH_2Cl_2 molecules (three per aggregate) = 288 e.

Crystallographic data (excluding structure factors) for the structures in this paper have been deposited with the Cambridge Crystallographic Data Centre as supplementary publication no. CCDC xxxxx. Copies of the data can be obtained, free of charge, on application to CCDC, 12 Union Road, Cambridge CB2 1EZ, UK: http://www.ccdc.cam.ac.uk/perl/catreq/catreq.cgi, e-mail: data_request@ccdc.cam.ac.uk, or fax: +44 1223 336033.

[x] G.M. Sheldrick, SHELXTL 6.14, Bruker AXS Inc., 6300 Enterprise Lane, Madison,WI 53719-1173, USA (2003)
[y]G.M. Sheldrick, SADABS 2.10 (the Siemens Area Detector Absorption Correction), University of Göttingen, (2005)
[z] Spek, A.L. (2003), J.Appl.Cryst. 36, 7-13

Magnetism:

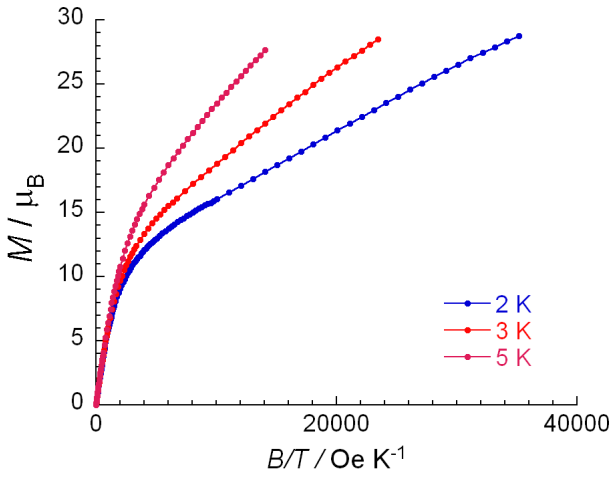

Figure S1. Magnetisation M vs applied field B against T at indicated temperatures.

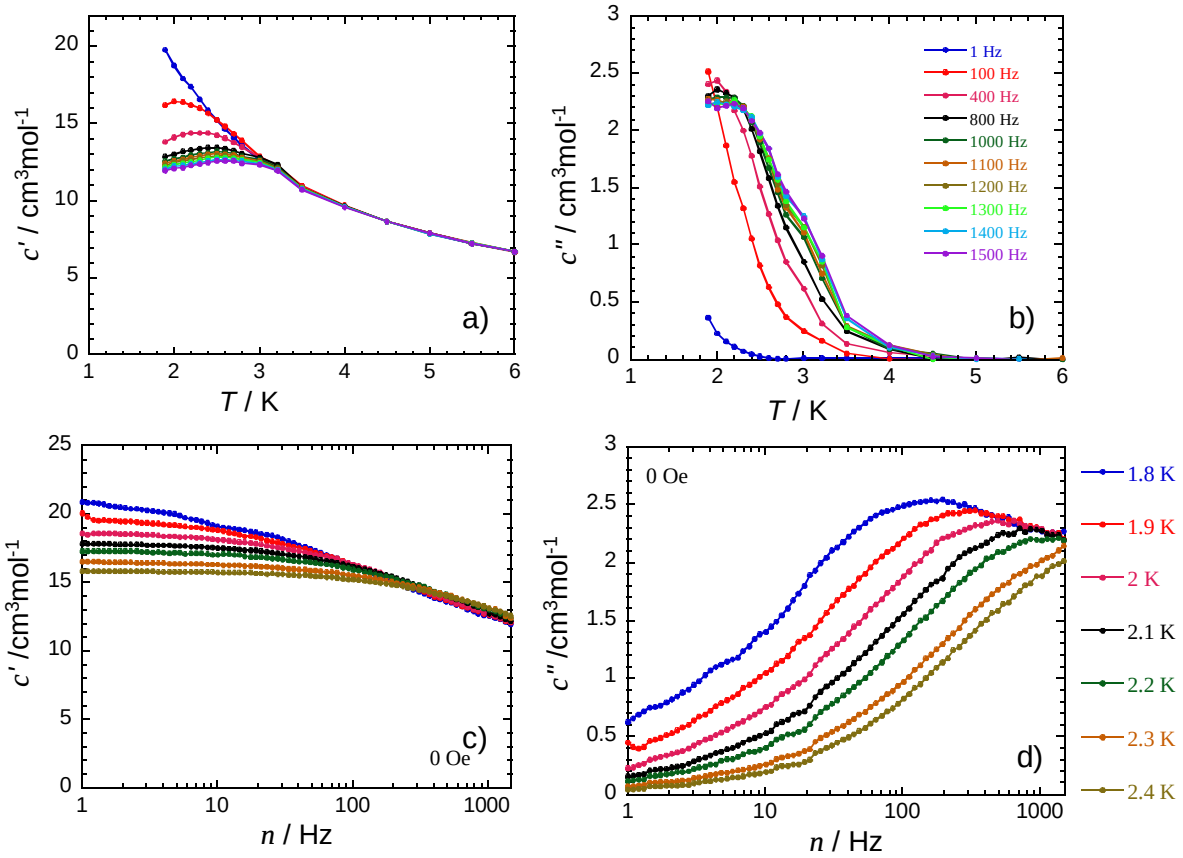

Figure S2. Temperature dependence of ac susceptibilities under zero dc field.

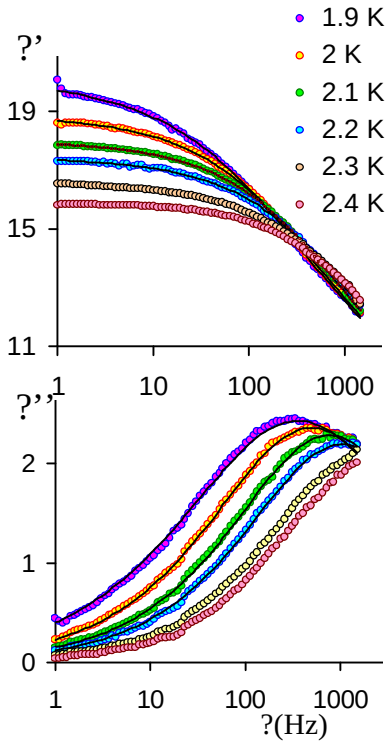

Figure S3. Plot of the frequency dependence of the ?' and ?'' susceptibility at indicated temperatures. The solid lines show the data fitted by least square methods.S1 and S2.

The complex susceptibility was phenomenologically expressed by modified Debye expressions (Cole-Cole equations):

$$c'(n_{ac}) = c_{\infty} + \frac{(c_0 - c_{\infty})\left[1 + (2pn_{ac}t)^{1-a}\sin(ap/2)\right]}{1 + 2(2pn_{ac}t)^{1-a}\sin(ap/2) + (2pn_{ac}t)^{2(1-a)}} \quad \text{(S1)}$$

$$c''(n_{ac}) = \frac{(c_0 - c_{\infty})\left[1 + (2pn_{ac}t)^{1-a}\cos(ap/2)\right]}{1 + 2(2pn_{ac}t)^{1-a}\sin(ap/2) + (2pn_{ac}t)^{2(1-a)}} \quad \text{(S2)}$$

The relative high value for a (0.42-0.5) indicate that more than one relaxation process is present at this temperature.

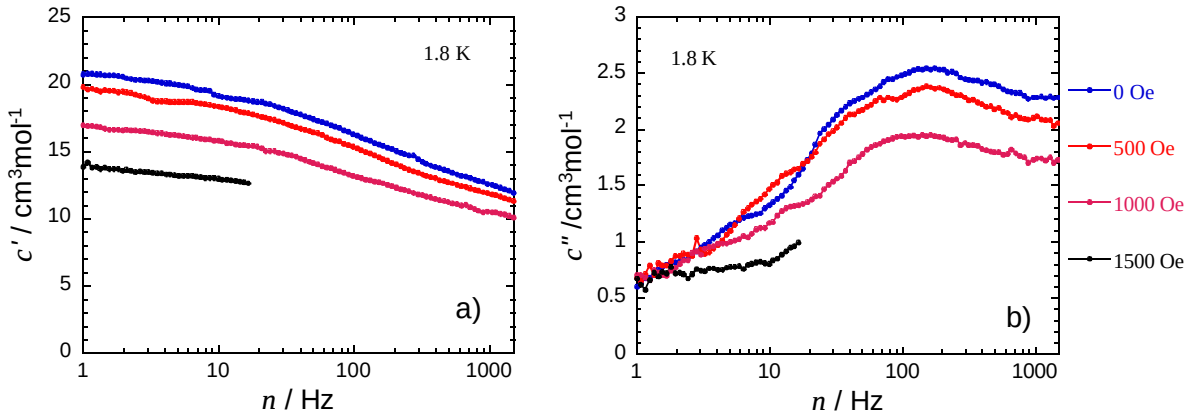

Figure S4. Frequency dependence of ac susceptibilities at 1.8 K under dc applied field.

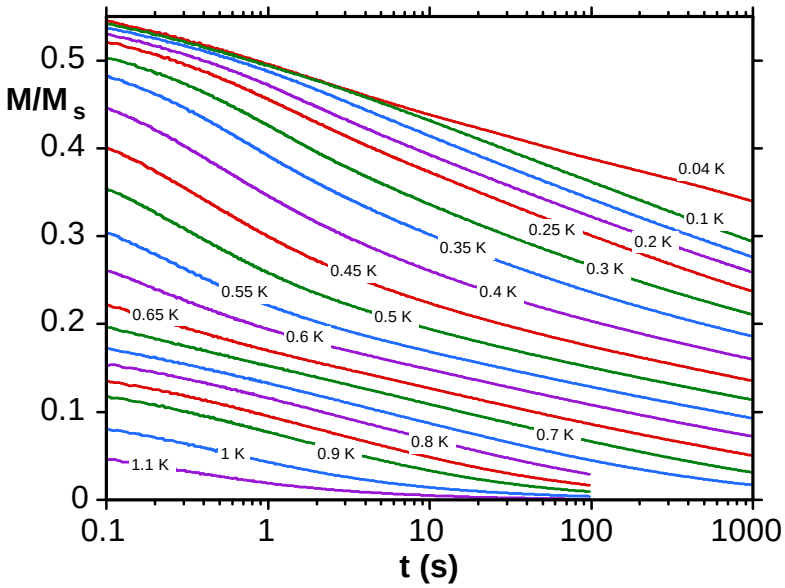

Figure S5 Magnetisation vs. time decay plots for a single crystal of **1** at the indicated temperatures.

Computational Details

The magnetic properties of metal centers in the Cr_4Dy_4 complex have been studied by fragment ab initio calculations by using a specially designed routine SINGLE_ANISO [1] interfaced with the MOLCAS package.[2] In this connection, the question arises to cut suitable mononuclear fragments from the molecule, which would not change significantly the energy structure on the magnetic centre. To have a good description of the 3d or 4f ligand-field states within a fragment one needs to take into account the influence of the neighbouring metal ions. To this end the neighbouring Dy^{3+} and Cr^{3+} have been simulated by the closed-shell La^{3+} ab initio embedding model potentials (AIMP) [3] and Zn^{2+}-AIMP.[3] or by ab initio effective core potentials (ECP) of La^{3+} and Sc^{3+} respectively. The latter approximation is generally expected to be better because the valence electrons of Sc^{3+} and La^{3+} are allowed to hybridize with the ligands' orbitals, which leads to a better description of the charge and covalence effects of the neighbouring Dy^{3+} and Cr^{3+}.

The second approximation concerned the coordination sphere. The structures of the calculated fragments are shown in Figures S6 and S7 below. No geometry optimisation on the fragments have been done, all atomic coordinates (except for added hydrogens) being taken from the crystal X-ray analysis. The basis sets used for the calculations were mainly taken from ANO-RCC and ANO-S basis libraries from MOLCAS package.[4]

For the electronic structure, the *ab initio* calculations were performed by means of MOLCAS-7.4 program.[2]

The active space for the complete active space self-consisting field (CASSCF) calculation of the dysprosium fragment included the 4f orbitals (CAS (9 in 7)) since we are interested in the ligand field states only. The active space for the CASSCF calculation of chromium fragment included three electrons in five 3d orbitals.

Since the lanthanides have a very strong spin-orbit coupling, a large number of roots should be included in the spin-orbit mixing within the restricted active space state interaction (RASSI-SO) procedure.[5] To avoid convergence problems we had to include in the self-consistent CASSCF calculation all possible roots available for a given active space, but we could mix by spin-orbit interaction only a limited amount of terms. We took in this mixing all roots up to 50000 cm^{-1}. An important aspect of the lanthanide state interaction calculation is that one should take into account all the states coming from an entire multiplet. Taking fewer roots may induce strong deviations, especially for low-lying multiplets. The number and free ion parentage of states mixed by RASSI are listed together with the fragment description below.

The second order multiconfigurational perturbation calculation (CASPT2) was performed only for chromium fragment. For dysprosium, due to the multitude of states needed to be mixed by spin-orbit coupling, the CASPT2 was too expensive computationally and was not done.

With the obtained spin-orbit multiplets, the powder susceptibility and the g-tensors for the lowest Kramers doublets of isolated fragments were further evaluated using the recently developed *ab initio* methodology.[1] The basis of this approach is the *ab initio* calculation of all orbital moment and magnetic moment matrix elements on the relevant spin-orbit multiplets obtained in CASSCF/CASPT2 calculations. These matrix elements are used in a separate routine to calculate:

(i) magnetic properties measured directly in experiment (temperature dependent Van Vleck susceptibility tensor and powder averaged function, field-dependent magnetisation for different temperatures and directions and the powder magnetisation) and

(ii) parameters of magnetic spin Hamiltonians for different spin-orbit multiplets and groups of spin states, described by the corresponding pseudospin, (*g* tensors, zero-field splitting tensors, etc).

In calculations of magnetic properties, all spin-orbit multiplets of ligand-field type on the metal sites are usually taken into account, in particular. This was found to be important for correct quantitative description of the effects of strong magnetic anisotropy and strong applied magnetic fields. Computationally, this routine (SINGLE_ANISO) was interfaced with MOLCAS-7.4 program.

CASSCF / CASPT2 calculations for metal fragments of Dy_4Cr_4 complex

Fragment Dy^{3+}

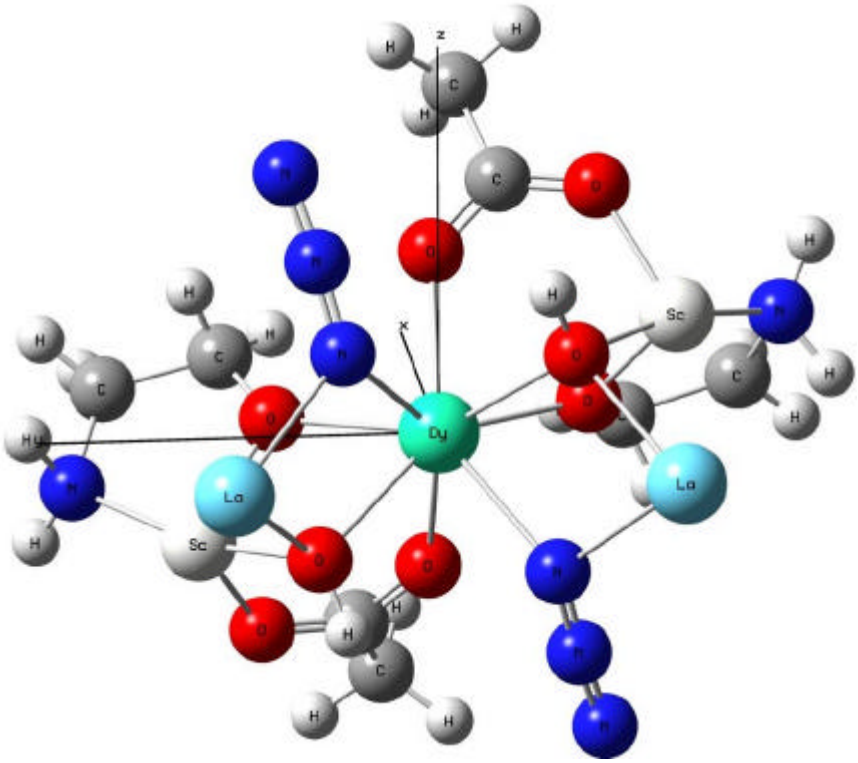

Figure S6*:* The structure of the calculated Dy^{3+} fragment.

Basis Sets

1. 427 basis functions:
ANO-RCC [8s7p5d4f2g1h] – for Dy^{3+}
ANO-RCC [3s2p1d] – for O and N from the first coordination sphere.
ANO-S [3s2p] – for C and distant O and N.

ANO-S [2s] – for H.
AIMP---La.ECP.deGraaf.0s.0s.0e-La(LaMnO3). – for Dy^{3+}.
AIMP---Zn.ECP.Lopez-Moraza.0s.0s.0e-AIMP-KZnF3. – for Cr^{3+}.
2. 722 basis functions:
ANO-RCC [9s8p6d4f3g2h] – for Dy^{3+}
ANO-RCC [4s3p2d1f] – for O and N from the first coordination sphere.
ANO-RCC [3s2p] – for C and distant O and N.
ANO-RCC [2s] – for H.
ECP--- La.ECP.Casarrubios.13s10p8d.1s2p2d.9e-CG-AIMP.– for Dy^{3+}.
ECP---Sc.ECP.Barandiaran.9s6p6d.1s2p2d.9e-CG-AIMP.– for Cr^{3+}.

Active space:
CAS(9 in 7).

Calculated roots:
All the states coming from the following multiplets have been taken into account in the spin-orbit interaction (RASSI): ^{6}H, ^{6}F, ^{6}P (all sextets), ^{4}I, ^{4}F, ^{4}M, ^{4}G, ^{4}L, ^{4}D, ^{4}H, ^{4}P, ^{4}G, ^{4}F, ^{4}I (128 out of 224 quartets), ^{2}L, ^{2}K, ^{2}P, ^{2}N, ^{2}F, ^{2}M, ^{2}H, ^{2}D, ^{2}G, ^{2}O (130 out of 490 doublets).

Table S1*:* Lowest calculated Kramers doublets, the ground g tensor and the angle of the main magnetic axis of the Dy^{3+} fragment with the Z axis of the complex in two different basis set approximations.

Nr.	Basis Set (nr. of basis functions)	States mixed in RASSI	Energy of eight lowest Kramers Doublets (cm^{-1})	*g* tensor of the ground KD	Angle of the main magnetic axis with Z axis of Dy_4Cr_4 (°)
1	427	279	0.000 28.204 56.383 76.426 128.115 175.043 216.091 545.695	g_x = 0.000156 g_y = 0.077320 g_z = 19.657181	36.98
2	722	279	0.000 23.343 65.207 101.897 155.451 271.375 357.537 682.658	g_x = 1.6671 g_y = 5.8397 g_z = 14.4195	20.06

Fragment Cr^{3+}

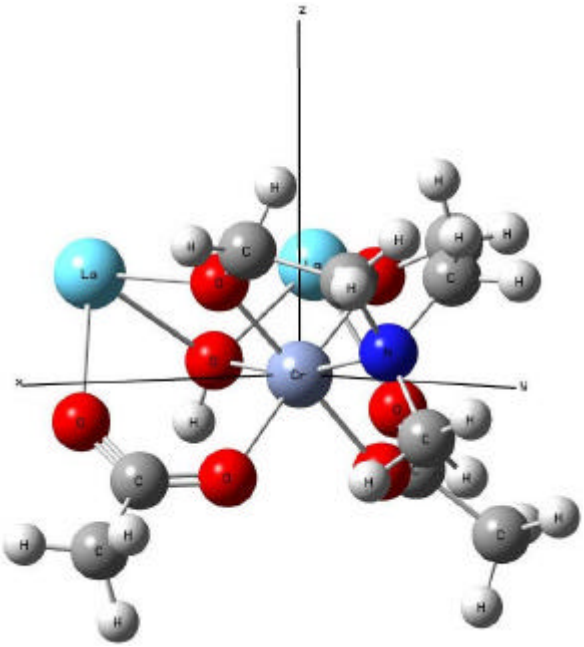

Figure S7*:* The structure of the calculated fragment containing Cr^{3+}.

Basis Sets
ANO-RCC [6s5p3d2f1g] – for Cr^{3+}.
ANO-RCC [3s2p1d] – for O and N.
ANO-S [3s2p1d] – for C.
ANO-S [2s1p] – for H.
ECP---La.ECP.deGraaf.0s.0s.0e-La(LaMnO3). – for Dy^{3+}.

Active space:
CAS(3 in 5).

Calculated roots:
^4F, ^4P, (all quartets); ^2H, ^2G, ^2F, ^2D, ^2D, ^2P (all doublets).

Table S2*:* Lowest calculated terms and Kramers doublets of the Cr^{3+} fragment.

	Spin Multiplicity	CASSCF / CASPT2 (cm^{-1})	Kramers doublets (cm^{-1})
1	4	0.000	0.000
2	4	16982.957	0.939
3	4	17460.181	16937.893
4	4	17596.071	16964.864
5	4	23303.635	17375.561
…	4	…	17432.931
1	2	18135.661	17530.520
2	2	18169.379	17597.383
3	2	18459.113	18119.567
4	2	18643.578	18270.558
5	2	19333.589	18530.363
6	2	26079.942	18712.525
7	2	27487.230	19356.205
8	2	28246.966	23318.289
9	2	32398.234	23325.888
10	2	34623.249	26074.185
…	2	…	…

Table S3: The g-tensor of the ground multiplet of Cr^{3+}.

	Spin-Orbit energy (cm^{-1})	g tensor of the ground $\tilde{S} = 3/2$	Magnetic Axes
1	0.000	g_x= 1.9636 g_y= 1.9677 g_z= 1.9684	0.0000 0.7410 -0.6715 -1.0000 0.0000 0.0000 0.0000 0.6715 0.7410

Simulation of the Magnetism of Dy_4Cr_4 complex in the limit of Ising exchange interaction between metal centers (basis set 1)

Ab initio calculations for the dysprosium fragment made with the basis set 1 (see the previous section) give highly anisotropic Dy^{III} ions, with $g_{||}$=19.657 and $g_{\perp}\approx 0$ in the ground Kramers doublet. The directions of anisotropy axes (shown in Figure S8a by red dashed lines) lie in the planes perpendicular to the twofold axes passing through the corresponding dysprosium ions and make an angle α with the common fourfold axis Z of the complex (Figure S8b).

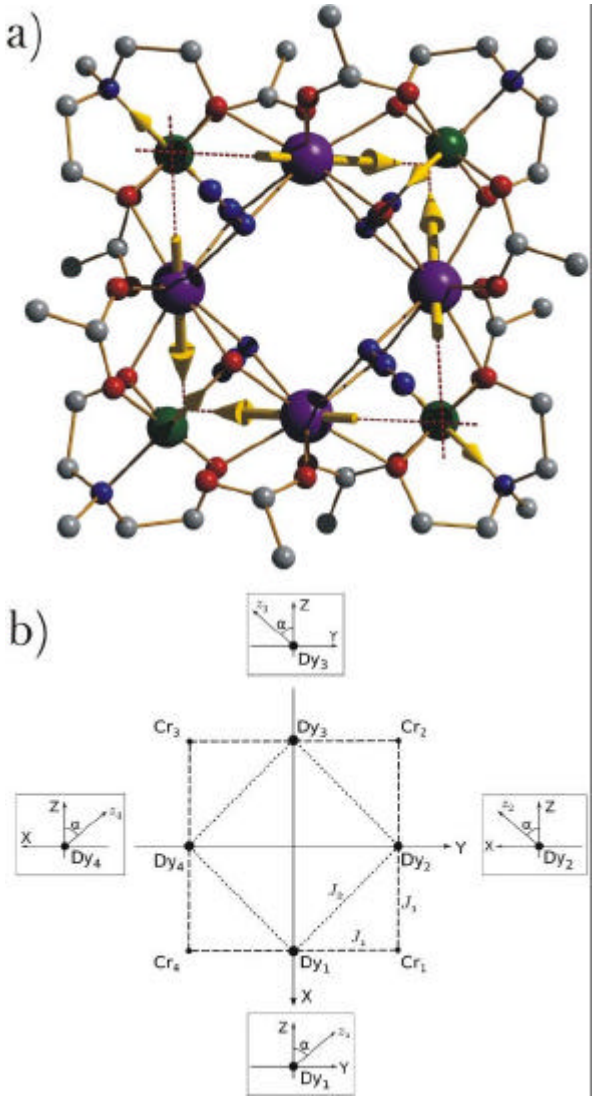

Figure S8. Directions of main anisotropy axes on Dy(III) (red dashed lines) and the direction of magnetic moments in the ground state of the complex (arrows).

On the contrary, the Cr^{III} ions are almost isotropic with g ≈ 1.97 (Table S3). Due to the high value of $g_{||}$ on the dysprosium ions, the exchange interaction amongst Dy(III) centres and with neighbouring chromium ions will be of the Ising type so that the total magnetic Hamiltonian for the lowest states is given by eq.(S1)

$$H = \sum_{i=1}^{4}\left[-J_1\left(s_i^{z_i}S_i^{z_i} + s_{i+1}^{z_{i+1}}S_i^{z_{i+1}}\right) - J_2 s_i^{z_i}s_{i+1}^{z_{i+1}} - m_B\left(g_{||}^{Dy}s_i^{z_i}B^{z_i} + g^{Cr}\vec{S}_i\cdot\vec{B}\right)\right] \qquad \text{(Eq. S1)}$$

where $s_i^{z_i}$ and $S_i^{z_i}$ are projections of the dysprosium *pseudo*spin s_i = 1/2 and chromium spin S_i = 3/2 on the anisotropy axis z_i of the Dy_i. $\vec{B}$ is the applied magnetic field and $\vec{B}^{z_i}$ is its projection on z_i.

?T at *T* = 0 is non-zero which means that the ground state of the whole complex is magnetic. This excludes the possibility of antiferromagnetic ordering of magnetic moments on the dysprosium ions. Ferromagnetic ordering of the dysprosium magnetic moments can be achieved for both signs of the interaction between Dy and Cr neighbors (J_1) as long as J_2 is not too negative. Interestingly, the value of *?T* at *T* = 0 does not depend on the absolute value of the exchange parameters, but only on the sign of J_1 and the angle *a* (Figure S8b), as given by eq. (S2):

$$cT\big|_{T\to 0} = \frac{N_A m_B^2}{3k}4\cos^2 a\left(g_{||}^{Dy} + \mathrm{sgn}(J_1)2\sqrt{2}g^{Cr}S\frac{1}{\sqrt{1+\cos^2 a}}\right)^2$$

Having in mind the overall antiferromagnetic behavior of susceptibility and using $g_{||}^{Dy} = 19.657$, close to the value Table S2 for basis set 1, the fitting of eq. (S2) gives $J_1 < 0$ and the value *a* = 49°. This value is higher than the one obtained in *ab initio* calculations (*a* = 37°), which can be due to the oversimplification of the model.

The simulations of the magnetic properties were done using eq. (S1), supplemented by the contributions from the local excited magnetic states on individual dysprosium and chromium sites extracted from CASSCF/CASPT2 (see Tables S1 (basis set 1) and S2) *ab initio* calculations.[6] Figure S9 shows the calculated *?T* and *M*(*B*) for a powder for J_1 = -10.1 cm^{-1} and J_2 = 6.8 cm^{-1}. We can see from the figure that the calculations reproduce the steep increase and the lack of saturation of magnetisation up to B = 7T. The values obtained for the exchange parameters give the ordering of magnetic moments in the ground state as shown in Figure S8a.

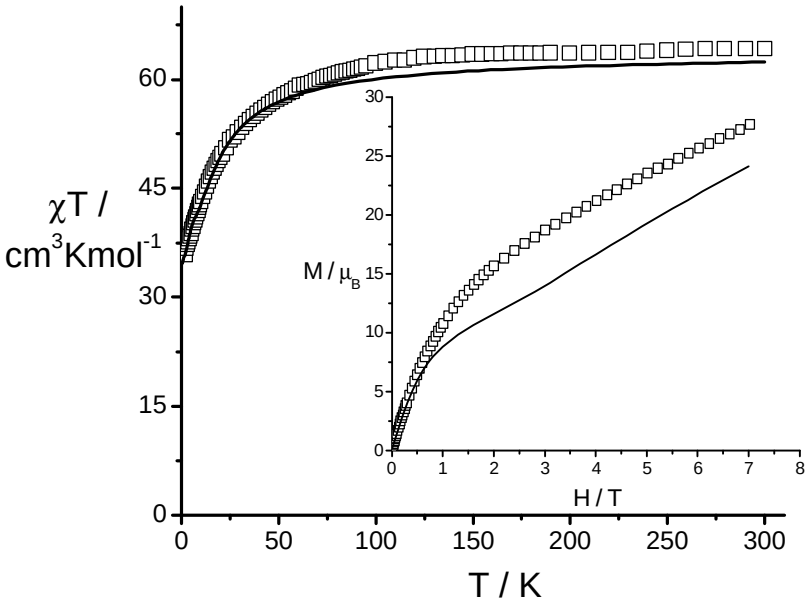

Figure S9. Temperature dependence of ?T under the applied field *H*= 0.1 T for **1** (squares) compared with that calculated using the parameters in the text. Inset: Experimental field-dependence of magnetisation at 5 K (squares) compared to the calculated curve.

Simulation of the Magnetism of Dy_4Cr_4 complex with an alternative set of Lines parameters (basis set 2)

In these simulations the Lines exchange parameters are taken as: J_1(Dy-Cr)=-1.50 c m^{-1}, J_2(Dy-Dy)=1.25 cm^{-1}, J_3(Cr-Cr)=-0.12 cm^{-1}.The results are shown in Figures S10 and S11.

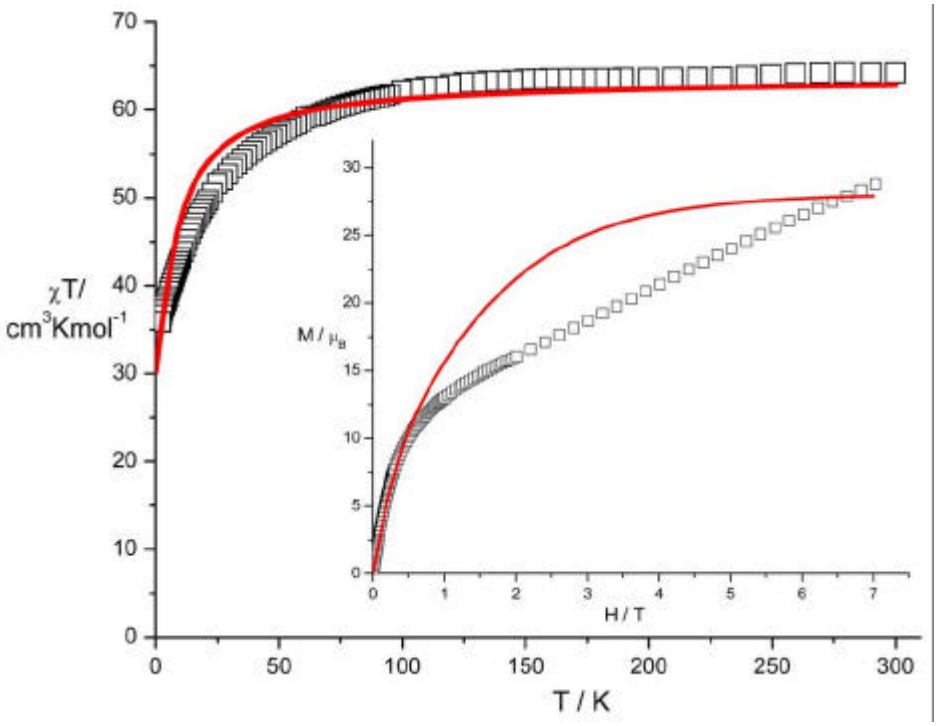

Figure S10. Temperature dependence of χT under 0.1 T applied field for **1** (squares) compared with that calculated (basis set 2) using the parameters set above. Inset: Experimental field-dependence of magnetisation at 2 K (squares) compared to the calculated curve.

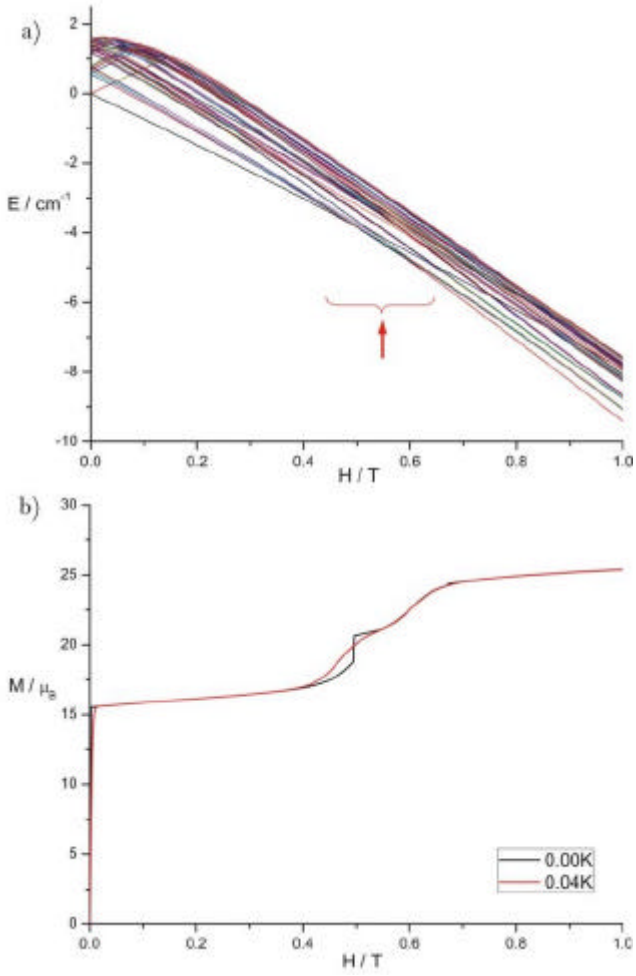

Figure S11. Evolution of the lowest energy levels (a) and the corresponding molar magnetisation (b) in the case when the magnetic field is applied along the main anisotropy axis (*Z*) of the Cr_4Dy_4 complex.

Although the magnetic susceptibility is explained satisfactorily and the magnetisation along the main anisotropy axis at T=0.04K shows a jump at fields H=0.4T-0.6T comparable to the experimental one (Figure 4b), the simulations do not reproduce correctly the field dependence of the powder molar magnetisation, which reaches saturation at 7T at variance with experiment. The reason for the obtained saturation of magnetisation is probably related to small values of exchange parameters used in these simulations. For larger exchange parameters the mean molar magnetisation does not reach saturation till 7T (cf Figures 2 and S9). Note the smeared magnetisation jump at T=0K, which is due to several and larger (compared to Fig. 6) avoided crossings of the ground state in the present simulations.

References

[1] L. F. Chibotaru, L. Ungur, Program SINGLE_ANISO, University of Leuven 2006.

[2] G. Karlström, R. Lindh, P. -Å. Malmqvist, B. O. Roos, U. Ryde, V. Veryazov, P. -O. Widmark, M. Cossi, B. Schimmelpfennig, P. Neogrady, L. Seijo, *Comp. Mater. Sci.* **2003**, *28*, 222-239.

[3] L. Seijo, Z. Barandiarán, in *Computational Chemistry: Reviews of Current Trends* **1999,** *4*, ed. by J. Leszcynski (World Scientific, Singapur), 55-152.

[4] K. Pierloot, B. Dumez, P.-O. Widmark and B. O. Roos, *Theor. Chim. Acta* **1995**, *90*, 87.; B. O. Roos, R. Lindh, P-O. Malmqvist,V. Veryazov V., P. O. Widmark, *J. Phys. Chem. A,* **2004**, *108*, 2851.

[5] B. O. Roos, P-O. Malmqvist, *Phys. Chem. Chem. Phys.* **2004**, *6*, 2919-2927.

[6] L. Ungur, W. Van den Heuvel, L.F. Chibotaru, *New J. Chem.* **2009**, *33*, 1224-1230.